# Manipulating Parallel and Perpendicular Multiphoton Transitions in $H_2$ Molecules

Shengzhe Pan,[1] Zhaohan Zhang,[2] Liang Xu,[2,3] Wenbin Zhang,[1] Peifen Lu,[1] Qinying Ji,[1] Kang Lin,[1] Lianrong Zhou,[1] Chenxu Lu,[1] Hongcheng Ni,[1,8] Camilo Ruiz,[4] Kiyoshi Ueda,[1,5] Feng He,[2,6,*] and Jian Wu[1,6,7,8,†]

[1]*State Key Laboratory of Precision Spectroscopy, East China Normal University, Shanghai 200241, China*
[2]*Key Laboratory for Laser Plasmas (Ministry of Education) and School of Physics and Astronomy, Collaborative Innovation Center of IFSA (CICIFSA), Shanghai Jiao Tong University, Shanghai 200240, China*
[3]*Shanghai Key Lab of Modern Optical System, University of Shanghai for Science and Technology, Shanghai 200093, China*
[4]*Instituto Universitario de Física Fundamental y Matemáticas, Universidad de Salamanca, Plaza de la Merced s/n, 37008 Salamanca, Spain*
[5]*Department of Chemistry, Tohoku University, Sendai 980-8578, Japan*
[6]*CAS Center for Excellence in Ultra-intense Laser Science, Shanghai 201800, China*
[7]*Chongqing Key Laboratory of Precision Optics, Chongqing Institute of East China Normal University, Chongqing 401121, China*
[8]*Collaborative Innovation Center of Extreme Optics, Shanxi University, Taiyuan, Shanxi 030006, China*

(Received 13 December 2022; revised 8 March 2023; accepted 16 March 2023; published 7 April 2023; corrected 10 May 2023)

We demonstrate that dissociative ionization of $H_2$ can be fully manipulated in an angle-time-resolved fashion, employing a polarization-skewed (PS) laser pulse in which the polarization vector rotates. The leading and falling edges of the PS laser pulse, characterized by unfolded field polarization, trigger, sequentially, parallel and perpendicular transitions of stretching $H_2$ molecules, respectively. These transitions result in counterintuitive proton ejections that deviate significantly from the laser polarization directions. Our findings demonstrate that the reaction pathways can be controlled through fine-tuning the time-dependent polarization of the PS laser pulse. The experimental results are well reproduced using an intuitive wave-packet surface propagation simulation method. This research highlights the potential of PS laser pulses as powerful tweezers to resolve and manipulate complex laser-molecule interactions.

DOI: 10.1103/PhysRevLett.130.143203

Tailoring ultrafast laser pulses makes it possible to manipulate ultrafast processes, such as breaking and forming molecular bonds in stereochemical reactions. Such pulse-shaped laser control technique leverages the interaction of the laser field with the molecule. In the case of linear molecules, the laser-molecule interactions depend on the angle between the laser field polarization and the molecular axis. This results in photon-coupled dipole transitions between various electronic states that can be classified into parallel and perpendicular transitions [1]. The former is favored when the laser polarization is parallel to the molecular axis, inducing electron transfer between two molecular orbitals with $\Delta\lambda = 0$, where $\lambda$ represents the orbital angular momentum projection along the molecular axis, while the latter is favored in a perpendicular case with $\Delta\lambda = \pm 1$. The parallel and perpendicular transitions occur in laser-molecule interactions and dominate the fundamental physical processes, such as the attosecond photoelectron emission delay [2–4], which can be further used to manipulate molecular reaction pathways [5–9], to enhance the coherent radiation [10–16], etc.

The control of parallel and perpendicular transitions towards switching ultrafast reaction pathways is highly desirable to be implemented in a coherent manner with subcycle precision. One of the simplest but very powerful techniques of tailoring the laser pulse, which may fulfill this requirement, is a generation of the shaped polarization-skewed (PS) laser pulse [17,18]. In the PS laser pulse, the polarization vector rotates from cycle to cycle and as a result the linear molecule experiences parallel and perpendicular transitions whose mixing ratio depends on its orientation with respect to the instantaneous field polarization of the PS pulse [see Fig. 1(a)]. Such PS laser pulses have been used for causing unidirectional rotational motion of molecules [17] and clocking ultrafast molecular ionizations [18–20], but so far have never been employed for controlling chemical reactions.

In the present Letter, we investigate parallel and perpendicular multiphoton transitions in dissociative ionization of $H_2$ molecules using PS laser pulses. Our results demonstrate the ability of the waveform-shaped PS pulses to control reaction pathways through the manipulation of hybrid parallel and perpendicular transitions. As depicted in Fig. 1(a), the application of PS laser pulses leads to the resolution and manipulation of reaction pathways, resulting in unexpected proton momentum distributions. A wave-packet surface propagation (WASP) simulation method with an intuitive physical scenario is utilized to uncover the underlying physical mechanisms that have never been examined so far in the multiphoton region and well reproduce the experimental observations.

 

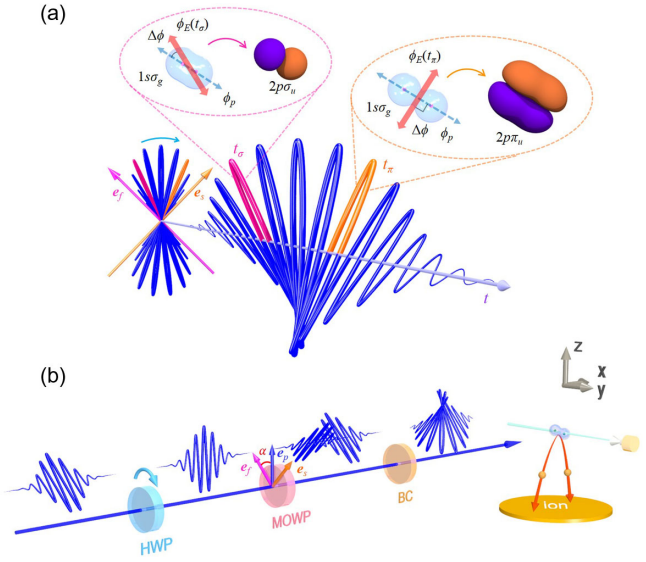


FIG. 1. (a) The sketch of the physical scenario. The linear molecule with the molecular axis along $\phi_p$ undergoes parallel ($1s\sigma_g$ to $2p\sigma_u$ state) and perpendicular ($1s\sigma_g$ to $2p\pi_u$ state) transitions at different instants when it experiences laser fields of different polarizations within a PS laser pulse. The two-dimensional fan-shaped structure on the left denotes the projection of the PS laser pulse perpendicular to the propagation direction. (b) Schematic illustrations of the experimental setup. The HWP is utilized to control the incident linear polarization of the UV laser pulse, as shown by a blue arrow (labeled as $\boldsymbol{e}_p$) before the MOWP, to manipulate the relative strength of two orthogonal components and thus the polarization waveform of the PS laser pulse. The constructed UV laser pulse is focused into the ultrahigh vacuum chamber, and protons are detected by a time- and position-sensitive detector.

Experimentally, as schematically illustrated in Fig. 1(b), a PS ultraviolet (UV) laser pulse is constructed by propagating a linearly polarized femtosecond laser pulse (54 fs, 395 nm) through a multiple-order wave plate (MOWP) in conjunction with a Berek compensator (BC) [17–20]. The time-dependent polarization evolution of the PS pulse is characterized by using polarization-resolved spectral interferometry [17]. The linearly polarized UV pulse is produced by frequency doubling the near-infrared femtosecond laser pulse delivered from a multipass Ti: sapphire laser system in a BBO crystal. The polarization of the PS UV laser pulse $\phi_E$ rotates from 135° (315°) to 45° (225°), shown by the light blue arrow in Fig. 1(a), in the $y$-$z$ plane defined by the orientation of the fast ($\boldsymbol{e}_f$, violet arrow) and slow ($\boldsymbol{e}_s$, yellow arrow) axes of the MOWP, which converts the incident linearly polarized pulse ($\boldsymbol{e}_p$, blue arrow) into two orthogonally polarized subpulses delayed in time in Fig. 1(b). For a given time lag ($\sim 32T$ with $T = 1.33$ fs being the optical cycle of the UV field used here), the polarization waveform of the PS laser pulse is determined by the projection of the incident linear pulse along the fast and slow axes of the MOWP, which can be finely adjusted by rotating the half-wave plate (HWP) before the MOWP. It tunes the relative strength of the leading and falling edges and thus the polarization waveform of the PS laser pulse. For instance, the blue fan-shaped inset of Fig. 1(a) plots the $y$-$z$ plane projection of the electric fields of the PS laser pulse when the linear polarization of the incident pulse is tuned to be along $\alpha = 45°$ with respect to the fast axis of the MOWP, as shown in Fig. 1(b). In our experiment, the peak intensity of the PS laser pulse when $\alpha = 0°$, i.e., a linearly polarized laser pulse, in the interaction region was calibrated to be $I_0 = 1 \times 10^{14}$ W/cm$^2$. The pulse energy of the incident UV pulse keeps unchanged when the crossing angle $\alpha$ is tuned in our experiment. The measurement is performed in an ultrahigh vacuum chamber of cold target recoil ion momentum spectrometer [21,22], where the protons produced from the strong-field dissociative (single and double) ionization of $H_2$ are detected by a time- and position-sensitive microchannel plate detector at the end of the spectrometer. Here, the axis of the $H_2$ molecule is randomly oriented in the jet, and the laser-field excitation selects molecules of preferential orientations to be eventually measured. The relatively slow rotation of the molecular axis is not considered here compared to the ultrafast dissociative ionization process.

Figure 2(a) displays the measured two-dimensional (2D) proton momentum distribution from the dissociative (single and double) ionization of $H_2$ driven by the PS laser field shown as the inset (left bottom). The P1 and P3 protons emitting to the directions of 45° (225°) $< \phi_p <$ 135° (315°), coinciding with the polarization-spanned electric field profile of the PS pulse, are produced via the parallel transition when the molecular axis is parallel to the laser polarization. Counterintuitively, there is a noticeable probability for molecules to dissociate along the direction apparently deviating from the laser polarization direction, i.e., the P2 and P2′ protons emitting to the directions around $\phi_p = 165°$ and 345°, which has never been observed previously in strong-field dissociative ionization of $H_2$. In the following, we first identify the various pathways and then explore the underlying physical mechanism governing the unforeseen distribution.

The protons with distinguished kinetic energy releases (KERs), as displayed in the inset of Fig. 2(a), are denoted as P1 (KER $<$ 1.8 eV), P2 (1.8 eV $<$ KER $<$ 3.0 eV), and P3 (KER $>$ 3.0 eV), which are produced via different reaction pathways and eject to different directions via parallel or perpendicular transitions. By comparing the proton KERs with that observed in a linearly polarized laser pulse [23–29], P1 and P3 are inferred to be the one-photon dissociation pathway of single and double ionization of $H_2$, respectively. As shown by the blue arrows in Fig. 2(b), for P1 and P3, the ionization-launched nuclear wave packet (NWP) moves outwards on the $1s\sigma_g$ curve and absorbs one photon at $R_1$, followed either by dissociation along the

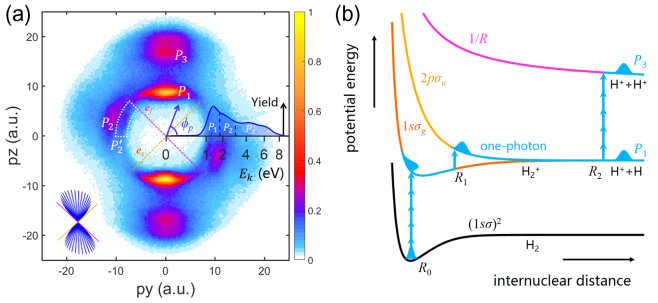


FIG. 2. (a) Measured momentum distribution of the protons driven by a PS UV laser pulse with $\alpha = 40°$ shown as the inset (left bottom). The violet and yellow dashed lines denote the fast ($\boldsymbol{e}_f$) and slow ($\boldsymbol{e}_s$) axes of the MOWP. The integrated KER spectrum is shown in the inset. (b) The schematic illustration of the one-photon dissociation pathway of single ionization (P1) and double ionization (P3). The neutral $H_2$ molecule is ionized at its equilibrium internuclear distance $R_0$, and the launched NWP moves outwards on the $1s\sigma_g$ curve and absorbs one photon at $R_1$, followed either by dissociation along the $2p\sigma_u$ curve, i.e., $H^+ + H$ (P1), or by further multiphoton ionization at $R_2$ and dissociation along the $1/R$ curve, i.e., $H^+ + H^+$ (P3). Multiple pathways via the parallel and/or perpendicular transitions to generate the unexpected P2 and P2′ protons are depicted in Fig. 3.

$2p\sigma_u$ curve, i.e., $H^+ + H$ (P1), or by further multiphoton ionization at $R_2$ and dissociation along the $1/R$ curve, i.e., $H^+ + H^+$ (P3). Since the one-photon transition between the $1s\sigma_g$ and $2p\sigma_u$ states is involved, the parallel transition is dominant and the proton ejections are consistent with the laser polarization directions as expected [30–33]. However, as shown in Fig. 2(a), the protons of P2 eject to the directions severely deviating from the laser polarization directions and from those perpendicular to them, which implies the participation of both the parallel and perpendicular transitions in the dissociative ionization of $H_2$ molecules, beyond all previous scenarios discovered in a linearly polarized laser pulse.

To reveal the underlying physics of the P2 proton ejections, we now discuss various routes via manipulating the time-dependent polarization of the PS laser pulse (the complete manipulation of reaction pathways as well as the polarization waveforms are shown in Supplemental Material [34]), looking into Fig. 3, where the experimental results are shown in the left inset of each panel and the relevant potential energy curves (including the $2p\pi_u$ state) are plotted. The KER of the P2 is similar to that of the direct dissociation pathway of double ionization of $H_2$ [26,27], which can be further classified into the *para* route, the *perp* route, and the *para-perp* route and can be angle-time resolved using a PS laser pulse. When $\alpha = 0°$, a linearly polarized laser pulse is constructed along the fast axis shown by the blue inset between the potential energy curves in Fig. 3(a). The P2 protons prefer to eject along the laser polarization direction, indicating that parallel transitions are involved. Since no net photon energy gain during the bond stretching is deduced from the KER of P2 protons, the process of absorbing a photon from the laser field and subsequently emitting another one, both in parallel transitions, should be involved by forming a complete dynamical Rabi coupling (same as the Rabi flopping of atoms) during bond stretching [35]. This process is favored near the internuclear distance where the one-photon resonant transition occurs for parallel-oriented molecules, highlighted by the blue up-down arrows around $R_1$ in Fig. 3(a). When the NWP propagates along the $1s\sigma_g$ curve to $R_2$, the $H_2^+$ molecule will be ionized via five-photon ionization and dissociate along the $1/R$ curve. This pathway may be named as the *para* route.

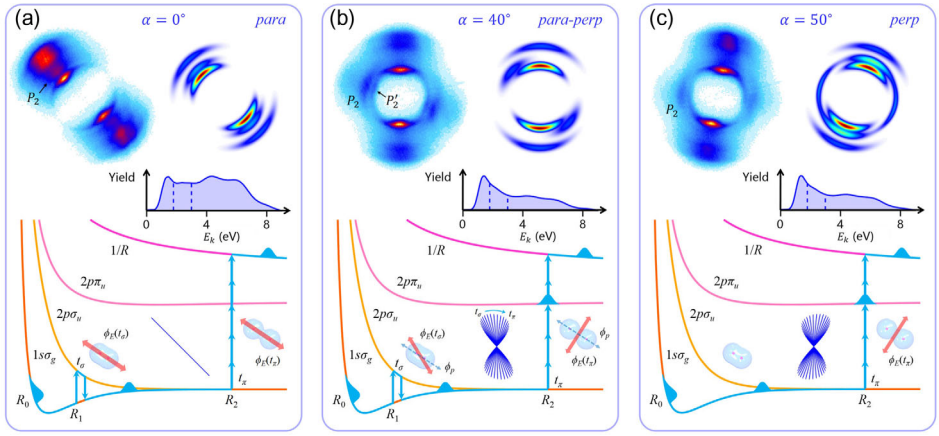


FIG. 3. Tunable PS laser pulses and corresponding anisotropic proton ejections in experiments and simulations. Here three typical waveforms are shown in the inset to illustrate the manipulation of the time-dependent polarization characteristic and the proton anisotropy. The corresponding measured KER spectra are depicted in the inset. The counterintuitive P2 protons are attributed to three different routes: (a) *para* route, (b) *para-perp* route, and (c) *perp* route. Three scenarios depict that the molecule undergoes parallel and/or perpendicular transitions at different instants when it experiences laser fields of different polarizations within a PS laser pulse.

For $\alpha = 40°$, as shown in Fig. 3(b), the laser field of the PS pulse is spanned temporally to form a fan-shaped profile. The $H_2^+$ molecule oriented around 165° experiences parallel transition at instant $t_\sigma$ in the leading edge of the PS pulse, as illustrated in Fig. 1(a), followed by absorbing three photons via the perpendicular transition and transiting from the $1s\sigma_g$ to $2p\pi_u$ state at instant $t_\pi$, highlighted by three blue up arrows at $R_2$ in Fig. 3(b). The NWP on the $2p\pi_u$ state has a great probability to be further ionized by absorbing two photons and to dissociate along the $1/R$ curve. This perpendicular transition has only been observed in the single-photon dissociation of perpendicular-oriented $H_2$ driven by XUV light [2,3,6,8]. Here we, for the first time, resolve the perpendicular multiphoton transition in $H_2$ by using a shaped PS laser pulse. Such a sequential parallel-perpendicular pathway, called the *para-perp* route, leads to unforeseen P2 proton ejections in the directions severely deviating from the laser polarization as shown in Figs. 2(a) and 3(b). Conversely, there is a small probability of the NWP remaining on the $2p\pi_u$ state, which ends up with slightly lower KER of the dissociative single ionization of $H_2$, labeled as P2′ in Fig. 2(a) and highlighted by the black arrow in Fig. 3(b).

For $\alpha = 50°$, the field strength in the falling edge of the PS pulse is stronger than the leading edge, as shown by the inset of Fig. 3(c). In this case, the leading edge of the PS pulse is not strong enough to induce the dynamical Rabi coupling and meanwhile, the falling edge can still excite the NWP to the $2p\pi_u$ state, followed by the subsequent two-photon ionization and Coulomb explosion, which may be named as the *perp* route. It produces the proton ejection around 180° labeled as P2, as shown in Fig. 3(c). Besides the *perp* route, the strong falling edge of the PS pulse acts as a linearly polarized field, still stimulating the *para* route and giving rise to the strong generation of P2 protons with the same directions as P1 and P3, which is even stronger than the *perp* route. The parallel or perpendicular transitions and the resulting proton KER spectra depend on the detailed waveform of the laser pulse, including the field strength, pulse duration, and time-dependent polarization. As shown in the inset of Fig. 3, although the KER peak positions of different pathways are almost the same, their relative strength and thus the profiles of the KER spectra change as a function of $\alpha$. Furthermore, by changing the time lag introduced by the MOWP and BC from 32 $T$ to 22 $T$, we found that the unexpected pathway of P2 disappeared.

To verify the aforementioned physical scenario, we perform numerical simulations using the WASP approach [36], which is efficient and intuitive in comparison to *ab initio* quantum simulation methods. The WASP approach is realized via the introduction of quantum elements including state transitions and phase accumulations into the classical propagation of the NWP on the potential energy surfaces of a stretching molecule [18–20,37–39]. The key of the WASP method is to construct the 2D dissociating NWP superimposed from various dissociation pathways, which can be written as

$$\psi(E_k, \phi_p, t_i) = \sum_J \psi_J(E_k, \phi_p, t_i) = \sum_J [G_J(E_k) A_J(\phi_p, t_i) e^{-i\varphi_J}], \quad (1)$$

where the kinetic energy $E_k$ and the molecular orientation $\phi_p$ define the 2D momentum space, $t_i$ is the instant of the first ionization, $\psi_J$ is the dissociating NWP for pathway $J$, $G_J$ is the Gaussian kinetic energy distribution, $A_J$ is the overall transition amplitude, and $\varphi_J$ is the accumulated phase.

The initial NWP is launched at the equilibrium internuclear distance of the neutral $H_2$ molecule upon electron removal at instant $t_i$, which is scanned over the entire laser pulse to match the experimental conditions. The subsequent propagation of the NWP on the potential energy curves of the $H_2^+$ cation is described as the classical motion of a particle with its reduced mass driven by the force $F = -dV(R)/dR$ [40], where $V(R)$ denotes the involved $1s\sigma_g$ or $2p\sigma_u$ potential energy curve labeled with its corresponding symmetry subscript, i.e., $V_g$ or $V_u$. When the NWP moves outwards to the photon-coupled resonant internuclear distance, it has a certain probability to absorb or emit photons and transit to other electronic states, including the parallel and perpendicular transitions, and subsequently, dissociate along new potential energy curves.

The single ionization probability $P_{SI}(t_i)$ is calculated according to the ADK theory [41]. For the aforementioned various reaction pathways, the typical *para-perp* route is taken as an example, where the parallel transition amplitude between the $1s\sigma_g$ and $2p\sigma_u$ state at $R_1$ can be approximately described as $A_\sigma = \Omega_{1\omega}\Omega_{\mathcal{R}}\tau_\sigma/\Delta V_{g\mathcal{R}}$ [36], and the perpendicular transition amplitude between the $1s\sigma_g$ and $2p\pi_u$ state at $R_2$ is described as $A_\pi = \Omega_{3\omega}^3\tau_\pi/4\omega^2$ [36,42]. Here, $\Omega_{1\omega} = D_{\sigma\sigma}(R_1)\mathcal{E}_\parallel(t)/2$ and $\Omega_{\mathcal{R}} = D_{\sigma\sigma}(R_{\mathcal{R}})\mathcal{E}_\parallel(t)/2$ denotes the dipole interactions between two $\sigma$ states when the NWP moves at the resonant distance $R_1$ and the Rabi coupling distance $R_{\mathcal{R}}$, respectively, $\Omega_{3\omega} = D_{\sigma\pi}(R_2)\mathcal{E}_\perp(t)/2$ denotes the dipole interaction between the $\sigma$ and $\pi$ states when the NWP moves to the resonant distance $R_2$, $\tau_\sigma$, and $\tau_\pi$ denote the effective duration of the two transitions in the molecular system, $\Delta V_{g\mathcal{R}} = -V_g(R_{1\omega}) + V_g(R_{\mathcal{R}})$ denotes the detuning of the subsequent Rabi coupling, and $4\omega^2$ denotes the detuning of the three-photon resonant transition. When the NWP is populated on the $2p\pi_u$ state, the $H_2^+$ will have a great probability of being ionized due to the small ionization potential, and the secondary ionization probability is approximately described as $P_{\mathrm{DI}}(t)$ using the ADK model. Thus, the whole transition amplitude of the *para-perp* route can be calculated as $A_{\sigma\pi} = A_\sigma A_\pi \sqrt{P_{\mathrm{SI}} P_{\mathrm{DI}}}$. Here

$\mathcal{E}_{\parallel} = E\cos(\phi_p - \phi_E)$ and $\mathcal{E}_{\perp} = E\sin(\phi_p - \phi_E)$ denote the projection of the laser electric field parallel and perpendicular to the molecular axis, respectively. During the bond stretching of the molecular ion, the NWP will accumulate a phase described as follows [36–38]:

$$\varphi_J = -\sum_{k=1}^{n} E_k \Delta t_k + \sum_{k=1}^{n-1}(-1)^k \omega_k t_k + \sum_{k=1}^{n-1}(-1)^{k-1}\pi + \int_{R_0}^{R_\infty} p_J(R)dR, \quad (2)$$

where the first term denotes the evolution phase of the nuclear eigenstate with the system energy $E_k$ and corresponding stretching time $\Delta t_k$, the second term denotes the evolution phase of the laser pulse with the absorption or emission of the photons of $\omega_k$, the third term denotes the phase associated with the symmetry change of the electronic wave function upon quantum-state transitions, and the last term denotes the dynamical phase of the NWP moving on the potential energy curves.

The WASP simulation can capture the essence of the classical and quantum elements in molecular dissociation and bring an intuitive physical picture. Numerically simulated momentum distributions of the ejected protons are depicted in the right inset of each panel in Fig. 3, which agree well with the experimental observations and verify the underlying processes of parallel and perpendicular multiphoton transitions in molecular dissociation. It is worth mentioning that the *para-perp* route dominates the generation of P2 when $\alpha = 40°$, for which the orthogonal laser field components at the leading and falling edges have similar field strengths. When $\alpha = 50°$, the leading edge of the PS laser pulse is weak, and so is the parallel transition at the leading edge, resulting in the suppression of the *para-perp* route and thus the appearance of the *perp* route. We further predict the contribution of the perpendicular transition in the circularly polarized laser pulse, which, however, is difficult to be picked out from the isotropic angular distribution of the ejected protons.

In conclusion, we have experimentally observed unforeseen proton ejections in dissociative double ionization of $H_2$ along the directions where the laser field vector is absent by using a PS UV laser pulse. It is found to be originating from the participation of the perpendicular multiphoton transition at the falling edge of the PS laser pulse following the parallel transition in the leading edge of the pulse. The participation of parallel and perpendicular transitions is further manipulated by finely controlling the time-dependent polarization of the PS laser pulse. The underlying physical scenarios are verified, and the experimental observations are well reproduced using the WASP simulation method. This phenomenon in $H_2$ observed here is general and applicable to other molecules with various electronic orbitals, and the time-dependent spatial polarization characteristic of the PS laser field opens new possibilities to observe and manipulate various strong-field dynamics of molecules.

We appreciate helpful discussions with Reinhard Dörner. This work was supported by the National Key R&D Program of China (Grant No. 2018YFA0306303 and No. 2018YFA0404802); the National Natural Science Foundation of China (Grants No. 11834004, No. 12227807, No. 12241407, No. 11925405, No. 91850203, No. 92150105, and No. 12204308); Science and Technology Commission of Shanghai Municipality (22ZR1444100).

*fhe@sjtu.edu.cn
†jwu@phy.ecnu.edu.cn

[1] B. H. Bransden and C. J. Joachain, *Physics of Atoms and Molecules*, 2nd ed. (Pearson, Singapore, 2003).
[2] L. Cattaneo, J. Vos, R. Y. Bello, A. Palacios, S. Heuser, L. Pedrelli, M. Lucchini, C. Cirelli, F. Martín, and U. Keller, Attosecond coupled electron and nuclear dynamics in dissociative ionization of $H_2$, Nat. Phys. **14**, 733 (2018).
[3] L. Cattaneo, L. Pedrelli, R. Y. Bello, A. Palacios, P. D. Keathley, F. Martín, and U. Keller, Isolating Attosecond Electron Dynamics in Molecules Where Nuclei Move Fast, Phys. Rev. Lett. **128**, 063001 (2022).
[4] X. Gong, W. Jiang, J. Tong, J. Qiang, P. Lu, H. Ni, R. Lucchese, K. Ueda, and J. Wu, Asymmetric Attosecond Photoionization in Molecular Shape Resonance, Phys. Rev. X **12**, 011002 (2022).
[5] Y. Nabekawa, Y. Furukawa, T. Okino, A. A. Eilanlou, E. J. Takahashi, K. Yamanouchi, and K. Midorikawa, Sub-10-fs control of dissociation pathways in the hydrogen molecular ion with a few-pulse attosecond pulse train, Nat. Commun. **7**, 12835 (2016).
[6] L. Martin, R. Y. Bello, C. W. Hogle, A. Palacios, X. M. Tong, J. L. Sanz-Vicario, T. Jahnke, M. Schöffler, R. Dörner, Th. Weber, F. Martín, H. C. Kapteyn, M. M. Murnane, and P. Ranitovic, Revealing the role of electron-electron correlations by mapping dissociation of highly excited $D_2^+$ using ultrashort XUV pulses, Phys. Rev. A **97**, 062508 (2018).
[7] D. You *et al.*, New Method for Measuring Angle-Resolved Phases in Photoemission, Phys. Rev. X **10**, 031070 (2020).
[8] D. S. Slaughter, F. P. Sturm, R. Y. Bello, K. A. Larsen, N. Shivaram, C. W. McCurdy, R. R. Lucchese, L. Martin, C. W. Hogle, M. M. Murnane, H. C. Kapteyn, P. Ranitovic, and Th. Weber, Nonequilibrium dissociative dynamics of $D_2$ in two-color, few-photon excitation and ionization, Phys. Rev. Res. **3**, 033191 (2021).
[9] C. Kleine, M.-O. Winghart, Z.-Y. Zhang, M. Richter, M. Ekimova, S. Eckert, M. J. J. Vrakking, E. T. J. Nibbering, A. Rouzée, and E. R. Grant, Electronic State Population Dynamics Upon Ultrafast Strong Field Ionization and Fragmentation of Molecular Nitrogen, Phys. Rev. Lett. **129**, 123002 (2022).
[10] H. Li, M. Hou, H. Zang, Y. Fu, E. Lötstedt, T. Ando, A. Iwasaki, K. Yamanouchi, and H. Xu, Significant Enhancement of $N_2^+$ Lasing by Polarization-Modulated

Ultrashort Laser Pulses, Phys. Rev. Lett. **122**, 013202 (2019).
[11] H. Li, E. Lötstedt, H. Li, Y. Zhou, N. Dong, L. Deng, P. Lu, T. Ando, A. Iwasaki, Y. Fu, S. Wang, J. Wu, K. Yamanouchi, and H. Xu, Giant Enhancement of Air Lasing by Complete Population Inversion in $N_2^+$, Phys. Rev. Lett. **125**, 053201 (2020).
[12] H. Li, S. Pan, F. Chen, F. Sun, Z. Li, H. Xu, and J. Wu, Optimization of $N_2^+$ lasing by waveform-controlled polarization-skewed pulses, Opt. Lett. **45**, 6591 (2020).
[13] M. Britton, M. Lytova, D. H. Ko, A. Alqasem, P. Peng, D. M. Villeneuve, C. Zhang, L. Arissian, and P. B. Corkum, Control of $N_2^+$ air lasing, Phys. Rev. A **102**, 053110 (2020).
[14] Y. Zhang, Z. Zhu, Y. Zheng, Y. Wu, Y. He, Z. Cui, B. Hu, P. Ding, and J. Ding, Optical gain in the P branch of $N_2^+$ lasing by polarization-modulated laser pulses, Phys. Rev. A **103**, 063110 (2021).
[15] S. Wang, E. Lötstedt, J. Cao, Y. Fu, H. Zang, H. Li, K. Yamanouchi, and H. Xu, Modulation of population inversion in $N_2^+$ by a pump-control-seed scheme, Phys. Rev. A **106**, 033110 (2022).
[16] H. Li, X. Gong, H. Ni, P. Lu, X. Luo, J. Wen, Y. Yang, X. Qian, Z. Sun, and J. Wu, Light-induced ultrafast molecular dynamics: from photochemistry to optochemistry, J. Phys. Chem. Lett. **13**, 5881 (2022).
[17] G. Karras, M. Ndong, E. Hertz, D. Sugny, F. Billard, B. Lavorel, and O. Faucher, Polarization Shaping for Unidirectional Rotational Motion of Molecules, Phys. Rev. Lett. **114**, 103001 (2015).
[18] Q. Ji, S. Pan, P. He, J. Wang, P. Lu, H. Li, X. Gong, K. Lin, W. Zhang, J. Ma, H. X. Li, C. Duan, P. Liu, Y. Bai, R. Li, F. He, and J. Wu, Timing Dissociative Ionization of $H_2$ Using a Polarization-Skewed Femtosecond Laser Pulse, Phys. Rev. Lett. **123**, 233202 (2019).
[19] S. Pan, C. Hu, Z. Zhang, P. Lu, C. Lu, L. Zhou, J. Wang, F. Sun, J. Qiang, H. Li, H. Ni, X. Gong, F. He, and J. Wu, Low-energy protons in strong-field dissociation of $H_2^+$ via dipole-transitions at large bond lengths, Ultrafast Sci. **2022**, 9863548 (2022).
[20] S. Pan, W. Zhang, H. Li, C. Lu, W. Zhang, Q. Ji, H. Li, F. Sun, J. Qiang, F. Chen, J. Tong, L. Zhou, W. Jiang, X. Gong, P. Lu, and J. Wu, Clocking Dissociative Above-Threshold Double Ionization of $H_2$ in a Multicycle Laser Pulse, Phys. Rev. Lett. **126**, 063201 (2021).
[21] R. Dörner, V. Mergel, O. Jagutzki, L. Spielberger, J. Ullrich, R. Moshammer, and H. Schmidt-Böcking, Cold target recoil ion momentum spectroscopy: a "momentum microscope" to view atomic collision dynamics, Phys. Rep. **330**, 95 (2000).
[22] J. Ullrich, R. Moshammer, A. Dorn, R. Dörner, L. P. H. Schmidt, and H. Schmidt-Böcking, Recoil-ion and electron momentum spectroscopy: reaction-microscopes, Rep. Prog. Phys. **66**, 1463 (2003).
[23] K. Sändig, H. Figger, and T. W. Hänsch, Dissociation Dynamics of $H_2^+$ in Intense Laser Fields: Investigation of Photofragments from Single Vibrational Levels, Phys. Rev. Lett. **85**, 4876 (2000).
[24] J. Wu, M. Kunitski, M. Pitzer, F. Trinter, L. P. H. Schmidt, T. Jahnke, M. Magrakvelidze, C. B. Madsen, L. B. Madsen, U. Thumm, and R. Dörner, Electron-Nuclear Energy Sharing in Above-Threshold Multiphoton Dissociative Ionization of $H_2$, Phys. Rev. Lett. **111**, 023002 (2013).
[25] X. Gong, P. He, Q. Song, Q. Ji, K. Lin, W. Zhang, P. Lu, H. Pan, J. Ding, H. Zeng, F. He, and J. Wu, Pathway-resolved photoelectron emission in dissociative ionization of molecules, Optica **3**, 643 (2016).
[26] P. Lu, W. Zhang, X. Gong, Q. Song, K. Lin, Q. Ji, J. Ma, F. He, H. Zeng, and J. Wu, Electron-nuclear correlation in above-threshold double ionization of molecules, Phys. Rev. A **95**, 033404 (2017).
[27] W. Zhang, X. Gong, H. Li, P. Lu, F. Sun, Q. Ji, K. Lin, J. Ma, H. Li, J. Qiang, F. He, and J. Wu, Electron-nuclear correlated multiphoton-route to Rydberg fragments of molecules, Nat. Commun. **10**, 757 (2019).
[28] H. Liang and L.-Y. Peng, Quantitative theory for electron-nuclear energy sharing in molecular ionization, Phys. Rev. A **101**, 053404 (2020).
[29] Z. Guo, Y. Fang, P. Ge, X. Yu, J. Wang, M. Han, Q. Gong, and Y. Liu, Probing tunneling dynamics of dissociative $H_2$ molecules using two-color bicircularly polarized fields, Phys. Rev. A **104**, L051101 (2021).
[30] L. J. Frasinski, J. Plumridge, J. H. Posthumus, K. Codling, P. F. Taday, E. J. Divall, and A. J. Langley, Counterintuitive Alignment of $H_2^+$ in Intense Femtosecond Laser Fields, Phys. Rev. Lett. **86**, 2541 (2001).
[31] P. Q. Wang, A. M. Sayler, K. D. Carnes, J. F. Xia, M. A. Smith, B. D. Esry, and I. Ben-Itzhak, Highlighting the angular dependence of bond softening and bond hardening of $H_2^+$ in an ultrashort intense laser pulse, J. Phys. B **38**, L251 (2005).
[32] A. Natan, M. R. Ware, V. S. Prabhudesai, U. Lev, B. D. Bruner, O. Heber, and P. H. Bucksbaum, Observation of Quantum Interferences via Light-Induced Conical Intersections in Diatomic Molecules, Phys. Rev. Lett. **116**, 143004 (2016).
[33] B. Fischer, M. Kremer, T. Pfeifer, B. Feuerstein, V. Sharma, U. Thumm, C. D. Schröter, R. Moshammer, and J. Ullrich, Steering the Electron in $H_2^+$ by Nuclear Wave Packet Dynamics, Phys. Rev. Lett. **105**, 223001 (2010).
[34] See Supplemental Material at http://link.aps.org/supplemental/10.1103/PhysRevLett.130.143203 for the animated movie to observe the complete manipulation of reaction pathways as well as the polarization waveforms of the PS laser pulses.
[35] S. Pan, C. Hu, W. Zhang, Z. Zhang, L. Zhou, C. Lu, P. Lu, H. Ni, J. Wu, and F. He, Rabi oscillations in a stretching molecule, Light Sci. Appl. **12**, 35 (2023).
[36] S. Pan, Z. Zhang, C. Hu, P. Lu, X. Gong, R. Gong, W. Zhang, L. Zhou, C. Lu, M. Shi, Z. Jiang, H. Ni, F. He, and J. Wu, Wave-packet surface propagation for light-induced molecular dissociation, arXiv:2303.13991.
[37] J. Wu, M. Magrakvelidze, L. Ph. H. Schmidt, M. Kunitski, T. Pfeifer, M. Schöffler, M. Pitzer, M. Richter, S. Voss, H. Sann, H. Kim, J. Lower, T. Jahnke, A. Czasch, U. Thumm, and R. Dörner, Understanding the role of phase in chemical bond breaking with coincidence angular streaking, Nat. Commun. **4**, 2177 (2013).
[38] S. Kangaparambil, V. Hanus, M. Dorner-Kirchner, P. He, S. Larimian, G. Paulus, A. Baltuška, X. Xie, K. Yamanouchi, F. He, E. Lötstedt, and M. Kitzler-Zeiler, Generalized Phase

Sensitivity of Directional Bond Breaking in the Laser-Molecule Interaction, Phys. Rev. Lett. **125**, 023202 (2020).
[39] Y. Mi, P. Peng, N. Camus, X. Sun, P. Fross, D. Martinez, Z. Dube, P. B. Corkum, D. M. Villeneuve, A. Staudte, R. Moshammer, and T. Pfeifer, Clocking Enhanced Ionization of Hydrogen Molecules with Rotational Wave Packets, Phys. Rev. Lett. **125**, 173201 (2020).
[40] I. A. Bocharova, A. S. Alnaser, U. Thumm, T. Niederhausen, D. Ray, C. L. Cocke, and I. V. Litvinyuk, Time-resolved Coulomb-explosion imaging of nuclear wave-packet dynamics induced in diatomic molecules by intense few-cycle laser pulses, Phys. Rev. A **83**, 013417 (2011).
[41] M. V. Ammosov, N. B. Delone, and V. P. Krainov, Tunnel ionization of complex atoms and atomic ions in an electromagnetic field, Sov. Phys. JETP **64**, 1191 (1986).
[42] V. M. Akulin and N. V. Karlov, *Intense Resonant Interactions in Quantum Electronics* (Springer-Verlag, Berlin, 1992).

*Correction:* The URL that enables access to the Supplemental Material was missing from Ref. [34] and has been inserted.